PAPER

Controlling the emission and absorption spectrum of a quantum emitter in a dynamic environment

IOP Publishing Journal of Physics B: Atomic, Molecular and Optical Physics
J. Phys. B: At. Mol. Opt. Phys. **52** (2019) 025501 (8pp) https://doi.org/10.1088/1361-6455/aaf452

Controlling the emission and absorption spectrum of a quantum emitter in a dynamic environment

H F Fotso

Department of Physics, University at Albany (SUNY), Albany, NY 12222, United States of America

E-mail: hfotso@albany.edu

Received 19 June 2018, revised 9 October 2018
Accepted for publication 27 November 2018
Published 14 December 2018

Abstract

We study the emission spectrum and absorption spectrum of a quantum emitter when it is driven by various pulse sequences. We consider the Uhrig sequence of nonequidistant π_x pulses, the periodic sequence of $\pi_x\pi_y$ pulses and the periodic sequence of π_z pulses (phase kicks). We find that, similar to the periodic sequence of π_x pulses, the Uhrig sequence of π_x pulses has emission and absorption that are, with small variations, analogous to those of the resonance fluorescence spectrum. In addition, while the periodic sequence of π_z pulses produces a spectrum that is dependent on the detuning between the emitter and the pulse carrier frequency, the Uhrig sequence of nonequidistant π_x pulses and the periodic sequence of $\pi_x\pi_y$ pulses have spectra with little dependence on the detuning as long as it stays moderate along with the number of pulses. This implies that they can also, similar to the previously studied periodic sequence of π_x pulses, be used to tune the emission or absorption of quantum emitters to specific frequencies, to mitigate inhomogeneous broadening and to enhance the production of indistinguishable photons from emitters in the solid state.

Keywords: emission/absorption spectrum, spectral diffusion, pulse-driven emitter, solid state emitter

(Some figures may appear in colour only in the online journal)

1. Introduction

Understanding the dynamics of a quantum emitter coupled to an electromagnetic field, in addition to being a longstanding fundamental question [1, 2], is also of significant current technological interest. In particular, the ability to control the emission or absorption spectrum of a quantum emitter will be of great value to the fields of quantum control, quantum metrology or quantum information processing (QIP) [3–6].

Indeed, many promising quantum systems that are prime candidates to serve as quantum bits (or qubits) in QIP are quantum emitters in the solid state [7–20]. As such, their emission and absorption spectra are subject to fluctuations in their environment that can lead to the spectrum drifting randomly in time: spectral diffusion [21, 22]. This phenomenon reduces the efficiency of fundamental operations in QIP such as the photon-mediated entanglement of distant quantum nodes or the coupling of quantum nodes to photonic cavities. It has for this reason received a great deal of attention [10–14, 21, 23–33].

In addition, the absorption spectrum of a quantum emitter such as a Nitrogen-vacancy (NV) center in diamond can be used to probe weak electromagnetic fields, temperatures or forces with very high spatial resolutions. Because of inhomogeneous broadening from the ensemble of emitters in the probe, the sensitivity is limited by $1/T_2^*$ instead of $1/T_2$ [34–36].

Recent work has explored the possibility of using adequate pulse sequences to control the spectrum of a quantum emitter [23, 37, 38]. In particular, it was shown that a periodic sequence of π_x pulses can be used to suppress spectral diffusion from photons produced by a quantum emitter in a diffusion-inducing environment thus enhancing photon indistinguishability [23]. The absorption spectrum of quantum

emitters subjected to the same pulse sequence was also studied theoretically [39] and experimentally shown to enhance the sensitivity of NV centers used in magnetometry to the $1/T_2$ limit [40].

These early studies focused on a periodic sequence of π_x pulses. The underlying mechanism for modifying the spectral lineshapes is clearly different from that of coherence protection with dynamical decoupling protocols. In the context of dynamical decoupling, the objective is to decouple the emitter from the decoherence inducing bath. In the current problem, our goal is not to decouple the emitter from the radiation bath, but rather to ensure emission/absorption at specific frequencies independent of the environment. However, in light of the similarities with dynamical decoupling where different pulse sequences are used with widely varying degrees of success, it is natural to inquire about the fate of the emission and absorption spectra of quantum emitters if they are driven by other pulse sequences. In this paper, we analyze the emission and absorption spectra of quantum emitters when they are driven by different other pulse sequences. We study the Uhrig sequence [41] of nonequidistant π_x pulses, the periodic sequence of π_x π_y pulses and the periodic sequence of π_z pulses.

We find that the Uhrig sequence of π_x pulses has emission and absorption spectra that are analogous to those of the resonance fluorescence spectrum. In particular, the emission spectrum, has a lineshape analogous to the Mollow triplet of a resonantly driven two-level system (TLS) [42–44] with most of the spectral weight at a central peak flanked with two satellite peaks; similarly, the absorption spectrum is similar to that of a TLS continuously driven on resonance and displays a local maximum at the pulse carrier frequency unlike that of the periodic sequence of π_x pulses that has a local minimum at the pulse carrier frequency. The periodic sequence of $\pi_x\pi_y$ pulses has emission and absorption spectra that are qualitatively different from those of π_x pulse protocols. They have their main peak at $\pi/2\tau$ and satellite peaks at $-\pi/2\tau$ and $\pi/2\tau + \pi/\tau$, where τ is the time interval between successive pulses. The periodic sequence of π_z pulses has a similar lineshape in both its emission and its absorption spectrum with two peaks of equal spectral weight at $\Delta - \pi/\tau$ and $\Delta + \pi/\tau$. Where Δ is the detuning between the emitter and the pulse carrier frequency. The Uhrig sequence of π_x pulses and the periodic sequence of $\pi_x\pi_y$ pulses have spectra with little dependence on the detuning of the emitter with respect to the pulse carrier frequency as long as it stays moderate along with the number of pulses. This implies that they can also be used to tailor the emission or absorption of quantum emitters, to mitigate inhomogeneous broadening and to enhance the production of indistinguishable photons from emitters in dynamic environments.

The rest of the paper is organized as follows. In section 2, we describe the model of the quantum emitter coupled to the radiation field and controlled by various pulse sequences, and the master equations governing the system dynamics. In section 3, we describe the methods used to obtain the emission and absorption spectra. In section 4 we present results that show the ability to tune the emission and absorption spectra with appropriate pulse sequences. Section 5 presents our conclusions.

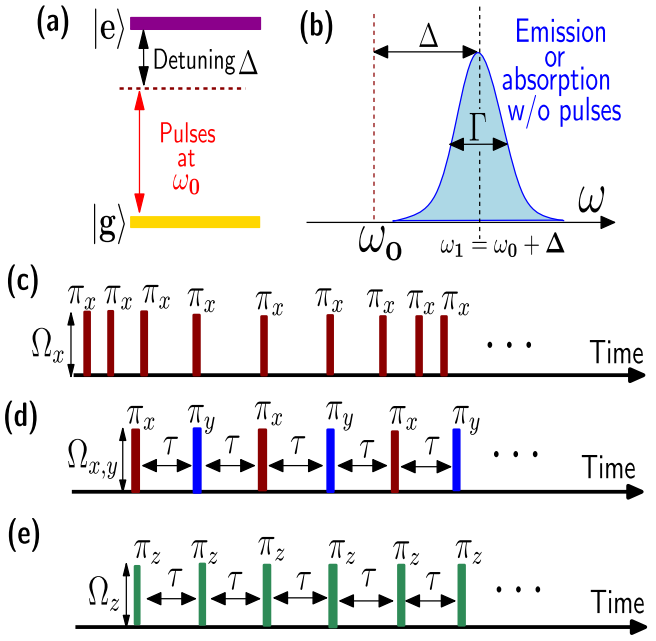

Figure 1. (a) Schematic representation of a two-level system with ground state $|g\rangle$ and excited state $|e\rangle$ separated by energy $\omega_1 = \omega_0 + \Delta$. (b) In the absence of any driving field, the emission and absorption spectra have a Lorentzian lineshape centered around ω_1. (c) Uhrig Sequence of π_x pulses. (d) Periodic sequence of $\pi_x\pi_y$ pulses. (e) Periodic sequence of π_z pulses.

2. Modeling the driven *emitter* + *radiation* system

The quantum emitter can be modeled as a TLS with ground state $|g\rangle$ and excited state $|e\rangle$, separated in energy by $E_e - E_g = \hbar\omega_1 = \hbar(\omega_0 + \Delta)$ (figure 1(a)). Below we set $\hbar = 1$. The TLS is coupled to normal modes of the electromagnetic radiation field, and is, at appropriate times, driven by pulses of the laser field with the Rabi frequency Ω. Initially, at time $t = 0$, the excited state is assumed to be occupied and the ground state to be empty; additionally, all bosonic modes are initially assumed to be empty. The Hamiltonian describing this system can be written as [45]:

$$H = \frac{\omega_1}{2}\sigma_z + \sum_k \omega_k a_k^\dagger a_k - i\sum_k g_k(a_k^\dagger\sigma_- - a_k\sigma_+) - \vec{d}\cdot\vec{E}_e. \quad (1)$$

The first term corresponds to the TLS, the second term to the radiation bath, the third term to the coupling between the TLS and the radiation bath written in the rotating-wave approximation (RWA). The last term corresponds to the coupling of the TLS with the external driving field. $\vec{d}$ is the electric dipole moment of the TLS and $\vec{E}_e$ is the external driving field that is applied at times prescribed by the pulse sequence. It has amplitude $\vec{\mathscr{E}}$ such that the Rabi frequency is $\Omega_i = \vec{d}\cdot\vec{\mathscr{E}}_i$. We have introduced the standard pseudo-spin Pauli operators for the TLS: $\sigma_z = |e\rangle\langle e| - |g\rangle\langle g|$, $\sigma_+ = |e\rangle\langle g|$ and

$\sigma_- = |g\rangle\langle e| = (\sigma_+)^\dagger$. $a_k^\dagger$ and a_k are respectively the creation and the annihilation operator for a photon of mode k with the frequency ω_k, and g_k is the coupling strength for this mode to the TLS.

For a given driving sequence, the last term of (1) can be expanded and written in the RWA. For π_x rotations, the relevant Hamiltonian is thus, in the frame rotating at frequency ω_0:

$$H = \sum_k \omega_k a_k^\dagger a_k + \frac{\Delta}{2}\sigma_z - i\sum_k g_k(a_k^\dagger \sigma_- - a_k\sigma_+) + \frac{\Omega_x(t)}{2}(\sigma_+ + \sigma_-), \tag{2}$$

where all energies are now measured with respect to ω_0 and $\Delta = \omega_1 - \omega_0$ is the detuning of the TLS's transition frequency from the pulse carrier frequency. The time-dependence $\Omega_x(t)$ is determined by the pulse sequence. We consider pulses such that $\Omega_i(t) = \Omega_i$ during the pulses and zero otherwise. We will assume Ω_i to be much larger than all other relevant energy scales so that the pulses are essentially instantaneous (i.e. $\Omega_i \gg \Delta, \Gamma, g_k$). Previous studies have shown that imperfect or finite width pulses do not significantly change the spectral lineshapes [23]. While the last term in (1), written in the form of (2), amounts to treating the incident field as a classical time-dependent field, it can be shown to be equivalent to the treatment of an initially coherent incident field via a unitary transformation [42, 45, 46].

In the absence of all control ($\Omega_i(t) = 0$ for all times), the system exhibits spontaneous decay, and the corresponding emission rate is $\Gamma = 2\pi\int g_k^2\,\delta(\omega_k - \Delta)\,dk$; We normalize our energy and time units so that $\Gamma = 2$, and the corresponding spontaneous emission line has a simple Lorentzian shape $1/(\omega^2 + 1)$, with the half-width equal to 1. This way, all frequencies are measured in units of $\Gamma/2$.

To characterize the dynamics of the system and obtain the emission and absorption spectrum, we analyze the time-evolution of the density matrix of the emitter, which is written as

$$\rho(t) = \rho_{ee}(t)|e\rangle\langle e| + \rho_{eg}(t)|e\rangle\langle g| + \rho_{ge}(t)|g\rangle\langle e| + \rho_{gg}(t)|g\rangle\langle g|, \tag{3}$$

with $\rho_{ge}^* = \rho_{eg}$. The master equations governing the time-evolution of the density matrix operator can be obtained from the Hamiltonian (2) by using the approximation of independent rate of variations whereby we independently add to the time-evolution of each matrix element of ρ, terms due to the radiation bath, the incident field and the damping terms responsible for spontaneous emission [45]. For π_x pulses and for the TLS described by the above Hamiltonian (2), the master equations in the rotating-wave approximation are:

$$\begin{aligned}
\dot\rho_{ee} &= i\frac{\Omega_x(t)}{2}(\rho_{eg} - \rho_{ge}) - \Gamma\rho_{ee},\\
\dot\rho_{gg} &= -i\frac{\Omega_x(t)}{2}(\rho_{eg} - \rho_{ge}) + \Gamma\rho_{ee},\\
\dot\rho_{ge} &= \left(i\Delta - \frac{\Gamma}{2}\right)\rho_{ge} - i\frac{\Omega_x(t)}{2}(\rho_{ee} - \rho_{gg}),\\
\dot\rho_{eg} &= \left(-i\Delta - \frac{\Gamma}{2}\right)\rho_{eg} + i\frac{\Omega_x(t)}{2}(\rho_{ee} - \rho_{gg}).
\end{aligned} \tag{4}$$

Each π_x pulse inverts the populations of the excited and ground state and swaps the values of ρ_{eg} and ρ_{ge}.

Similarly, each π_y pulse inverts the populations of the excited and ground states and swaps the values of ρ_{eg} with $-\rho_{ge}$ and vice versa. We will also consider π_z pulses that are equivalent to π phase kicks leaving ρ_{ee} and ρ_{gg} unchanged and replacing ρ_{eg} by $-\rho_{eg}$ and ρ_{ge} by $-\rho_{ge}$. In general, the effect of a π_i pulse can be summarized as:

$$\rho^{(n)}(0^+) = \sigma_i\rho^{(n)}(0^-)\sigma_i, \tag{5}$$

where $\rho^{(n)}(0^-)$ and $\rho^{(n)}(0^+)$ are the density matrices immediately before and immediately after the n^{th} pulse. σ_i is the pseudo-spin Pauli matrix in the i-direction in which the pulse applies the rotation.

The emission spectrum can be obtained using a narrow-band detector that can be modeled as a two-level absorber with a very sharp transition frequency [47]. The excitation probability of this detector then corresponds to the emission spectrum. At long times T, it can be expressed as:

$$P(\omega) = 2A^2 \times \mathrm{Re}\left\{\int_0^T dt\int_0^{T-t} d\theta\,\langle\sigma_+(t+\theta)\sigma_-(t)\rangle\exp[-i\omega\theta]\right\}. \tag{6}$$

$\sigma_-(t)$ and $\sigma_+(t+\theta)$ are the time-dependent operators in the Heisenberg representation, and the angled brackets represent the expectation values that are taken with respect to the initial state of the TLS (in our case, fully occupied excited state and empty ground state). The constant A is independent of the pulse parameters, does not affect the spectral shape and only affects the absolute scale of the spectrum.

On the other hand, the absorption spectrum considered here is measured by determining the energy absorbed from a weak probing field by the TLS while it is simultaneously being driven by the relevant pulse sequence. Since the probing field is assumed to be weak enough that its effects on the populations of the states can be neglected, the absorption spectrum can be calculated within the linear response theory. The absorption as a function of frequency, $Q(\omega)$, is given by [48, 49]

$$Q(\omega) = 2A^2 \times \mathrm{Re}\left\{\int_0^T dt\int_0^{T-t} d\theta\,\langle[\sigma_-(t),\,\sigma_+(t+\theta)]\rangle\,\mathrm{e}^{-i\omega\theta}\right\}, \tag{7}$$

$[O_1, O_2]$ is the commutator of the operators O_1 and O_2. For the absorption spectrum, the expectation value is evaluated in

the absence of the probing field. The expression (7) can be rewritten as

$$\begin{aligned} Q(\omega) &= 2A^2\,\mathrm{Re}\,\{\mathcal{P}_2(\omega) - \mathcal{P}_1(\omega)\} \\ &= P'(\omega) - P(\omega), \end{aligned} \tag{8}$$

where

$$\mathcal{P}_2(\omega) = \int_0^T dt \int_0^{T-t} d\theta\, \langle \sigma_-(t)\sigma_+(t+\theta)\rangle \mathrm{e}^{-i\omega\theta} \tag{9}$$

and

$$\mathcal{P}_1(\omega) = \int_0^T dt \int_0^{T-t} d\theta\, \langle \sigma_+(t+\theta)\sigma_-(t)\rangle \mathrm{e}^{-i\omega\theta}. \tag{10}$$

The term $P(\omega) = 2A^2\,\mathrm{Re}\,\{\mathcal{P}_1(\omega)\}$ can be recognized to be the emission spectrum of equation (6). $P'(\omega) = 2A^2\,\mathrm{Re}\,\{\mathcal{P}_2(\omega)\}$ can be viewed as the direct absorption so that the difference yields the net absorption [42]. To obtain the absorption spectrum, both terms are evaluated independently before then taking the difference to obtain $Q(\omega)$.

In the absence of any pulses, as illustrated in figure 1(b), the emission spectrum and absorption spectrum have Lorentzian-shaped profiles centered at the emitter's frequency that is equal to the detuning Δ (in the frame rotating at ω_0).

The two-time correlation function $\langle \sigma_+(t+\theta)\sigma_-(t)\rangle$ that appears in the expression for the emission spectrum $P(\omega)$ is usually expressed as a single-time expectation value [2, 42, 47] following:

$$\begin{aligned} &\langle \sigma_+(t+\theta)\sigma_-(t)\rangle \\ &= \mathrm{Tr}\,[\rho(0)U^\dagger(0,t+\theta)\sigma_+U(0,t+\theta)U^\dagger(0,t)\sigma_-U(0,t)] \end{aligned} \tag{11}$$

$$= \mathrm{Tr}\,[\sigma_-\rho(t)U^\dagger(t,t+\theta)\sigma_+U(t,t+\theta)] \tag{12}$$

$$= \mathrm{Tr}\,[\rho'(t+\theta)\sigma_+] \tag{13}$$

where $\rho'(t) = \sigma_-\rho(t)$, and where σ_+ and σ_- are the time-independent operators in the Schrödinger picture. $U(t,t')$ is the time-evolution operator for the system described by equations (4). Similarly, to evaluate $P'(\omega)$, we rewrite the involved two-time correlation function as:

$$\langle \sigma_-(t)\sigma_+(t+\theta)\rangle = \mathrm{Tr}\,[\sigma_+\rho''(t+\theta)] \tag{14}$$

with $\rho''(t) = \rho(t)\sigma_-$.

3. Analytical and numerical solutions

The expectation values (13) and (14), and the emission and absorption spectra, can be evaluated numerically, or for simple pulse sequences, analytically. Both methods, as demonstrated previously [39], are in perfect agreement.

While the analytical solution of the master equation is in general rather tedious, for a periodic sequence of instantaneous pulses, one obtains a set of decoupled first order differential equations that can be solved in a procedure similar to that of [39] where the obtained analytical solution was also shown to overlap with the numerical solution. Alternatively, one can also, in this case of periodic instantaneous pulses, integrate the Heisenberg equations of motion in a toggling frame. We outline this solution here for the calculation of the emission spectrum of a quantum emitter driven by a periodic sequence of $\pi_x\pi_y$ pulses. In this situation, the Hamiltonian after the nth pulse can be rewritten as:

$$\begin{aligned} H(t) &= (-1)^n\frac{\Delta}{2}\sigma_z + \sum_k \omega_k a_k^\dagger a_k \\ &+ i\sum_k g_k\{\chi_1 a_k^\dagger\sigma_- - \chi_1 a_k\sigma_+ + \chi_2 a_k^\dagger\sigma_+ - \chi_2 a_k\sigma_-\}, \end{aligned} \tag{15}$$

where $\chi_1(t) = \xi_1(t) - \xi_3(t)$ and $\chi_2(t) = \xi_2(t) - \xi_4(t)$ with $\xi_{1,2,3,4}$ periodic functions defined in the interval $[0, 4\tau]$ by:

$$\text{for } 0 < t < \tau;\quad \xi_1(t) = 1,\quad \xi_{2,3,4}(t) = 0, \tag{16}$$

$$\text{for } \tau < t < 2\tau;\quad \xi_2(t) = 1,\quad \xi_{1,3,4}(t) = 0, \tag{17}$$

$$\text{for } 2\tau < t < 3\tau;\quad \xi_3(t) = 1,\quad \xi_{1,2,4}(t) = 0, \tag{18}$$

$$\text{for } 3\tau < t < 4\tau;\quad \xi_4(t) = 1,\quad \xi_{1,2,3}(t) = 0. \tag{19}$$

From the above Hamiltonian, one obtains after the nth pulse the equations of motion:

$$\dot{a}_k = -i\omega_k a_k + g_k(\chi_1\sigma_- + \chi_2\sigma_+) \tag{20}$$

$$\dot{\sigma}_- = -i(-1)^n\Delta\sigma_- + \sum_k g_k\chi_1 a_k\sigma_z - \sum_k g_k\chi_2 a_k^\dagger\sigma_z \tag{21}$$

$$\dot{\sigma}_z = -2\sum_k g_k[\chi_1 a_k^\dagger\sigma_- + \chi_1 a_k\sigma_+ - \chi_2 a_k^\dagger\sigma_+ - \chi_2 a_k\sigma_-]. \tag{22}$$

Starting from an initial configuration at $t = 0$ in which all bosonic modes are empty and the emitter has its excited state fully occupied and its ground state empty, we want to evaluate the number $N_k = \langle a_k^\dagger(t)a_k(t)\rangle$ of bosons in bosonic mode k at time $t = N\tau + \delta$ where N is a multiple of 4 and $\delta \in [0, \tau]$. To this end, we will recursively integrate the above equations of motion for the annihilation operator a_k after successive pulses. After N pulses, employing the Markovian approximation, we will get:

$$\begin{aligned} a_k^{(N)}(t) &= a_k(0)\mathrm{e}^{-i\omega_k t} + g_k\int_{N\tau}^{t}\sigma_-^{(N)}(t_1)\mathrm{e}^{-i\omega_k(t-t_1)}dt_1 \\ &+ g_k\sum_{l=0}^{N/4-1}\int_0^{4\tau}\chi_1(t_2)\sigma_-^{(l)}(t_2)\mathrm{e}^{-i\omega_k(t-t_2-4l\tau)}dt_2 \\ &+ g_k\sum_{l=0}^{N/4-1}\int_0^{4\tau}\chi_2(t_2)\sigma_+^{(l)}(t_2)\mathrm{e}^{-i\omega_k(t-t_2-4l\tau)}dt_2. \end{aligned} \tag{23}$$

To be able to utilize this expression, we now need to obtain $\sigma_{-,+}$ after each pulse interval. Within the Markovian approximation, integrating for $\sigma_-(\tau)$ gives:

$$\sigma_-(\tau) = \mathrm{e}^{-i(\Delta\tau + i\gamma^{(0)}(\tau))}\sigma_-(0) \tag{24}$$

with $\gamma^{(0)}(\tau) = \sum_k g_k^2\frac{\tau}{i(\omega_k-\Delta)} - \sum_k g_k^2\frac{\mathrm{e}^{-i(\omega_k-\Delta)\tau}-1}{(\omega_k-\Delta)^2}$. Similarly, integrating for $\sigma_-(2\tau)$ will give:

$$\sigma_-(2\tau) = \mathrm{e}^{i(\Delta\tau + i\gamma^{(0)*})}\sigma_-(\tau) \tag{25}$$

$$= \mathrm{e}^{i(\Delta\tau + i\gamma^{(0)*})}\mathrm{e}^{-i(\Delta\tau + i\gamma^{(0)})}\sigma_-(0) \tag{26}$$

$$= \mathrm{e}^{2\,i\,\mathrm{Im}(\gamma^{(0)})}\sigma_-(0). \tag{27}$$

Here, one immediately notices the cancellation of Δ between (26) and (27). This is the aforementioned phase cancellation that is responsible for the spectrum not depending on the detuning with respect to the pulse-carrier frequency. This cancellation is due to the change of sign in the first term of the Hamiltonian of equation (15) between consecutive pulses.

By proceeding in this iterative integration, one obtains, for an integer $n < N/2$:

$$\sigma_-(2n\tau) = \mathrm{e}^{i\{2n\ \mathrm{Im}\,\gamma^{(0)}\}}\sigma_-(0), \tag{28}$$

$$\sigma_-((2n+1)\tau) = \mathrm{e}^{\{i\ 2n\ \mathrm{Im}\,\gamma^{(0)}+\gamma^{(0)}-i\Delta\tau\}}\sigma_-(0). \tag{29}$$

We also get after the Nth pulse:

$$\sigma_-^{(N)}(t) = \sigma_-(0)\mathrm{e}^{iN\,\mathrm{Im}\,(\gamma^{(0)}(\tau))}\mathrm{e}^{-i(\Delta(t-N\tau)+i\phi(t-N\tau))} \tag{30}$$

with $\phi(t) = \sum_k g_k^2\left[\frac{t-N\tau}{i(\omega_k-\Delta)} - \frac{\mathrm{e}^{-i(\omega_k-\Delta)(t-N\tau)}-1}{(\omega_k-\Delta)^2}\right]$.

These expressions, along with the corresponding expressions for σ_+ can then be plugged into equation (23) allowing for the evaluation of the emission spectrum in terms of expectation values at time $t = 0$. Making use of $\sigma_-\sigma_+ = (I-\sigma_z)/2$ and $\sigma_+\sigma_- = (I+\sigma_z)/2$ and of the vanishing of expectation values of $\sigma_-\sigma_-$ and $\sigma_+\sigma_+$, the nonzero terms can be collected into a straightforward but lengthy expression that will not be displayed here. These nonzero terms can then be evaluated numerically and summed up to produce the spectrum. The resulting spectrum has a lineshape that is, with respect to peak positions and relative spectral weights, consistent with that obtained by either analytical or numerical solution of the master equation.

For the numerical solution of the master equation (4), the time axis is divided in finite pulse intervals separated by consecutive pulses, and each pulse interval is discretized in smaller steps of length Δt. Starting at $t = 0$, with the known initial conditions, $\rho_{ee} = 1$, $\rho_{gg} = 0$, $\rho_{eg} = 0$, $\rho_{ge} = 0$, we integrate equation (4) to evolve the matrix elements ρ_{ee}, ρ_{eg}, ρ_{ge}, ρ_{gg} from time t to $t+\Delta t$ and iterate this integration up to the first pulse time T_1. We then apply the pulse to the system (i.e equation (5) to the density matrix operator) before resuming the iterative integration starting from time T_1 and up to T_2, the time at which the next pulse is applied. This process is repeated until time $T_{N_p} = T$ where N_p is the total number of pulses. It allows us to obtain, $\rho'(t)$ and $\rho''(t)$ for $t \in [0, T]$. We can then proceed, once again, with the integration of equation (4) starting at $t \in [0, T]$ to obtain $\rho'(t+\theta)$ and $\rho''(t+\theta)$ for $\theta \in [0, T-t]$. It is thereon straightforward to obtain $\langle\sigma_+(t+\theta)\sigma_-(t)\rangle$ and $\langle\sigma_-(t)\sigma_+(t+\theta)\rangle$ from equations (13) and (14) respectively. We finally get the emission spectrum and the absorption spectrum by performing the relevant Fourier transforms with respect to θ and integration over t to get $\mathcal{P}_1(\omega)$ and $\mathcal{P}_2(\omega)$. The real part of $\mathcal{P}_1(\omega)$ gives the emission spectrum and the difference between the real parts of $\mathcal{P}_2(\omega)$ and $\mathcal{P}_1(\omega)$ gives the absorption spectrum. The results that we present next are obtained using this numerical approach that treats all pulse sequences on the same footing.

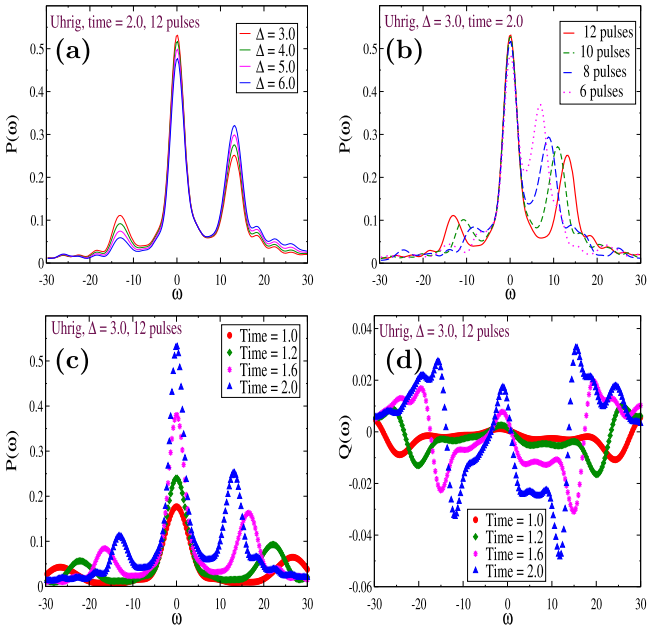

Figure 2. Emission and absorption spectra of TLS driven by a Uhrig sequence of π_x pulses. (a) Emission for different values of the detuning Δ between the transition frequency and the pulse carrier frequency ($\Delta = 3.0$ (red), $\Delta = 4.0$ (green), $\Delta = 5.0$ (magenta), $\Delta = 6.0$ (blue)) after 12 pulses applied during time $T = 2.0$. (b) Emission for fixed detuning ($\Delta = 3.0$) with 6 pulses (doted magenta line), 8 pulses (dashed blue line), 10 pulses (dashed green line), 12 pulses (red line) after time $T = 2.0$. (c) Emission for fixed detuning ($\Delta = 3.0$) with 12 pulses applied during a total time $T = 1.0$ (red circles), $T = 1.2$ (green diamonds), $T = 1.6$ (magenta stars), $T = 2.0$ (blue triangles). (d) Absorption for fixed detuning ($\Delta = 3.0$) with 12 pulses applied during a total time $T = 1.0$ (red circles), $T = 1.2$ (green diamonds), $T = 1.6$ (magenta stars), $T = 2.0$ (blue triangles).

4. Results

4.1. Uhrig pulse sequence

The Uhrig pulse sequence was recently suggested as a sequence of nonequidistant pulses that is optimal in preventing decoherence due to low frequency noise in the environment [41]. A cycle of the Nth order Uhrig pulse sequence is made of N pulses applied at times given by:

$$T_j = T\sin^2\frac{j\pi}{2(N+1)}, \quad \text{with} \quad j = 1, 2, \cdots, N. \tag{31}$$

The $(N+1)$th pulse is applied at $T_{N+1} = T$ and the time sequence is repeated. The Uhrig pulse sequence is illustrated in figure 1(c). Considering the importance of this pulse sequence in the dynamical decoupling context, it is is useful to study how it affects the emission or absorption spectrum of a quantum emitter in a diffusion-inducing bath. In figure 2, we present results for a quantum emitter driven by a Uhrig sequence of π_x pulses. The emission spectrum is found to have a central peak at the pulse carrier frequency, flanked by two satellite peaks the position of which is dependent on the number of pulses. The emission and absorption spectra do not depend much on the detuning Δ as long as it remains moderate (figures 2(a)–(c)). For the same detuning Δ and fixed

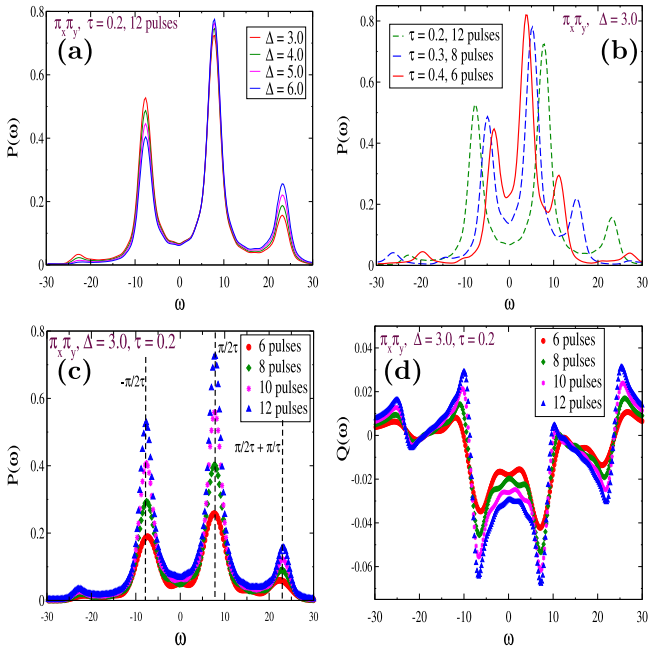

Figure 3. Emission and absorption spectra of TLS driven by a periodic sequence of π_x π_y pulses. (a) Emission for different values of the detuning Δ between the transition frequency and the pulse carrier frequency ($\Delta = 3.0$ (red), $\Delta = 4.0$ (green), $\Delta = 5.0$ (magenta), $\Delta = 6.0$ (blue)) after 12 pulses with a time spacing $\tau = 0.2$ between successive pulses. (b) Emission for fixed detuning ($\Delta = 3.0$) with 6 pulses and $\tau = 0.4$ (red line), 8 pulses and $\tau = 0.3$ (dashed blue line), 12 pulses and $\tau = 0.2$ (dashed green line). (c) Emission for fixed detuning ($\Delta = 3.0$) and $\tau = 0.2$ after 6 pulses (red circles), 8 pulses (green diamonds), 10 pulses (magenta stars), 12 pulses (blue triangles). (d) Absorption for fixed detuning ($\Delta = 3.0$) after 6 pulses (red circles), 8 pulses (green diamonds), 10 pulses (magenta stars), 12 pulses (blue triangles).

time T, the central peak is of similar spectral weight and satellite peaks move further away from it as the number of pulses increases (figure 2(b)). We note a strong analogy with the spectrum of the resonance fluorescence problem. The absorption spectrum has both positive and negative parts with the former often interpreted as true absorption and the latter as stimulated emission in the direction of the probing field [48, 50, 51]. Markedly, the absorption spectrum has a local maximum at the pulse carrier frequency (figure 2(d)) unlike that of a periodic sequence of π_x pulses that has a local minimum at the pulse carrier frequency.

4.2. π_x π_y pulse sequence

In figure 3, we present the results for an emitter driven by a periodic sequence of $\pi_x\pi_y$ pulses. The emission spectrum has its main peak located at $\pi/2\tau$ with additional peaks at $-\pi/2\tau$ and $\pi/2\tau + \pi/\tau$ (figure 3(c)) unlike the periodic sequence of π_x pulses for which the main peak is at the pulse carrier frequency ($\omega = 0$ in the frame rotating at the pulse carrier frequency). For fixed detuning, the τ-dependence of the emission spectrum is shown in figure 3(b). The lineshape is established early and the peaks grow in amplitude with time (figure 3(c)). The absorption spectrum has its main dip at $\pi/2\tau$ and two additional dips at $-\pi/2\tau$ and $\pi/2\tau + \pi/\tau$ (figure 3(d)). Both the emission and the absorption spectra show little dependence on Δ for moderate values of the pulse spacing time τ as long as $\Delta \lesssim 1/\tau$ (figure 3(a)).

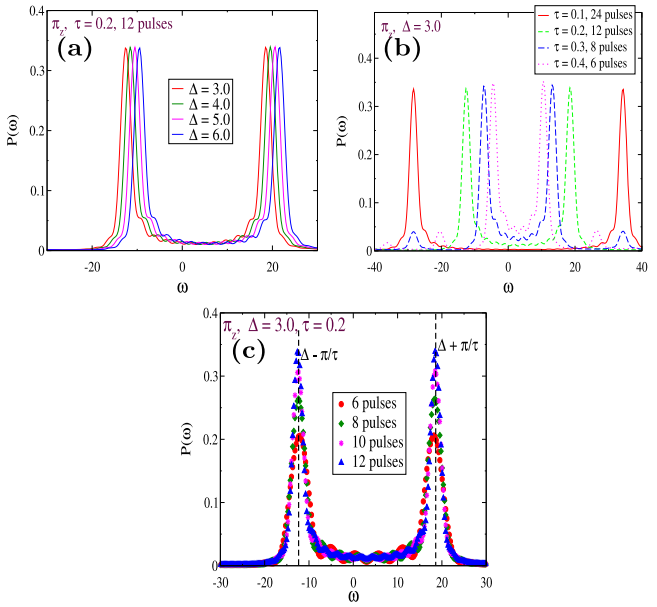

Figure 4. Emission spectrum of TLS driven by a periodic sequence of π_z pulses (phase kicks). (a) For different values of the detuning Δ between the transition frequency and the pulse carrier frequency ($\Delta = 3.0$ (red), $\Delta = 4.0$ (green), $\Delta = 5.0$ (magenta), $\Delta = 6.0$ (blue)) after 12 pulses with a time spacing $\tau = 0.2$ between successive pulses. (b) For fixed detuning ($\Delta = 3.0$) with 6 pulses and $\tau = 0.4$ (doted magenta line), 8 pulses and $\tau = 0.3$ (dashed blue line), 12 pulses and $\tau = 0.2$ (dashed green line), 24 pulses and $\tau = 0.1$ (red line). (c) For fixed detuning ($\Delta = 3.0$) and $\tau = 0.2$ after 6 pulses (red circles), 8 pulses (green diamonds), 10 pulses (magenta stars), 12 pulses (blue triangles).

4.3. π_z pulse sequence

Contrary to the π_x and the $\pi_x\pi_y$ pulse sequences, a sequence of π_z pulses (or π phase kicks), produces a spectrum that depends on the detuning between the pulse carrier frequency and the TLS frequency (4(a)). This can be related to the fact that the toggling frame Hamiltnian in this case does not display a sign change between consecutive pulses such as that of π_x or π_y pulses that is seen in equation (15). Both the absorption spectrum and the emission spectrum have similar lineshapes. Thus we only present in figure 4 the emission spectrum for π_z pulses. The emission spectrum is split in two peaks of equal weight located at $\Delta - \pi/\tau$ and $\Delta + \pi/\tau$ (4(b)–(c)). Thus, for the same pulse sequence, it depends strongly on the values of Δ (figure 4(a)). These results are in agreement with those of [37] where a model of the *atom + radiation* system was solved using direct diagonalization for a finite but large number of bosonic modes.

5. Conclusions

We have studied the emission and absorption spectra of a quantum emitter when it is driven by a pulse sequence.

Representing the quantum emitter as a TLS, we have used the master equation governing the time-evolution of the density matrix operator of the pulse-driven system to obtain the spectrum for the different protocols. We have considered the case of the Uhrig sequence of π_x pulses, a periodic sequence of π_x π_y pulses and a periodic sequence of π_z phase kicks. In the absence of any driving protocol, the emission and absorption spectra have Lorentzian lineshapes centered around the frequency $\Delta = E_e - E_g$ (measured in the frame rotating at the target frequency ω_0). The periodic sequence of π_z phase kicks splits the emission spectrum in two peaks of equal weight at $\Delta + \pi/\tau$ and $\Delta - \pi/\tau$. It also modifies the absorption spectrum in a similar manner. The Uhrig sequence of π_x pulses has an emission and absorption spectrums similar to that of a periodic sequence of π_x pulses where a central peak with the bulk of the emission/absorption appears at the pulse carrier frequency with satellite peaks at positive and negative frequencies dependent on the number of pulses. In addition, its absorption spectrum displays a strong analogy with that of the resonance fluorescence with a peak (a maximum) at the pulse carrier frequency as opposed to the minimum that is observed for the periodic sequence of π_x pulses. The periodic sequence of π_x π_y pulses produces an emission spectrum with the main peak located at $\pi/2\tau$ and satellite peaks at $-\pi/2\tau$ and $\pi/2\tau + \pi/\tau$. Similarly, for the Uhrig sequence of π_x pulses, the spectra show little dependence on the detuning for a moderate number of pulses over the emission time. These results provide a detailed picture for the emission and absorption spectra of a quantum emitter when it is driven by different pulse sequences. They also indicate that the Uhrig pulse sequence and the periodic sequence of $\pi_x\pi_y$ pulses can be used to control the effect of the environment on the emission and absorption spectrum. As highlighted in the analytical solution, the phase cancellation responsible for the limited dependence of the spectrum on the environment will occur as long as the detuning with respect to the pulse carrier frequency and the time between consecutive pulses remain moderate (for periodic pulses: $\Delta \cdot \tau \sim 1$). Most importantly, this phase cancellation argument is made with no additional regard to the underlying mechanism responsible for the fluctuations in Δ. This suggests that these results can be observed in a variety on quantum emitters. For instance, 3 to 4 pulses per free emission time should suffice for NV centers in diamond.

Acknowledgments

We thank V V Dobrovitski for inspiring this work and for insightful discussions. We thank V Mkhitaryan for helpful discussions.

ORCID iDs

H F Fotso https://orcid.org/0000-0001-7952-6256

References

[1] Heitler W 1960 *The Quantum Theory of Radiation* 3rd edn (Oxford: Oxford University Press)
[2] Loudon R 1983 *The Quantum Theory of Light* (Oxford: Clarendon)
[3] Kimble H J 2008 *Nature* **453** 1023
[4] Walmsley I and Rabitz H 2003 *Phys. Today* **56** 43
[5] Braginsky V B, Khalili F Y and Thorne K S 1992 *Quantum Measurement* (Cambridge: Cambridge University Press)
[6] Nielsen M A and Chuang I L 2000 *Quantum Computation and Quantum Information* (Cambridge: Cambridge University Press)
[7] Imamoğlu A, Awschalom D D, Burkard G, DiVincenzo D P, Loss D, Sherwin M and Small A 1999 *Phys. Rev. Lett.* **83** 4204
[8] Childress L, Taylor J M, Sørensen A S and Lukin M D 2006 *Phys. Rev. Lett.* **96** 070504
[9] Hanson R and Awschalom D D 2008 *Nature* **453** 1043
[10] Bernien H *et al* 2013 *Nature* **497** 86
[11] Pfaff W *et al* 2014 *Science* **345** 6196
[12] Gao W B, Fallahi P, Togan E, Delteil A, Chin Y S, Miguel-Sanchez J and Imamoglu A 2013 *Nat. Commun.* **4** 2744
[13] Hensen B *et al* 2015 *Nature* **526** 682
[14] Basset L C, Heremans F J, Yale C G, Buckley B B and Awschalom D D 2011 *Phys. Rev. Lett.* **107** 266403
[15] Faraon A, Barclay P E, Santori C, Fu K-M C and Beausoleil R G 2011 *Nat. Photon.* **5** 301
[16] Doherty M W, Manson N B, Delaney P, Jelezko F, Wrachtrup J and Hollenberg L C L 2013 *Phys. Rep.* **528** 1
[17] Sipahigil A, Jahnke K D, Rogers L J, Teraji T, Isoya J, Zibrov A S, Jelezko F and Lukin M D 2014 *Phys. Rev. Lett.* **113** 113602
[18] Rogers L J *et al* 2014 *Phys. Rev. Lett.* **113** 263602
[19] Santori C, Fattal D, Vučković J, Solomon G S and Yamamoto Y 2002 *Nature* **419** 594
[20] Carter S G, Sweeney T M, Kim M, Kim C S, Solenov D, Economou S E, Reinecke T L, Yang L, Bracker A S and Gammon D 2013 *Nat. Photon.* 29
[21] Fu K-M C, Santori C, Barclay P E, Rogers L J, Manson N B and Beausoleil R G 2009 *Phys. Rev. Lett.* **103** 256404
[22] Ambrose W P and Moerner W E 1991 *Nature* **349** 225
[23] Fotso H F, Feiguin A E, Awschalom D D and Dobrovitski V V 2016 *Phys. Rev. Lett.* **116** 033603
[24] Hansom J, Schulte C H H, Matthiesen C, Stanley M J and Atatüre M 2014 *Appl. Phys. Lett.* **105** 172107
[25] Acosta V M *et al* 2012 *Phys. Rev. Lett.* **108** 206401
[26] Kuhlmann A V, Houel J, Ludwig A, Greuter L, Reuter D, Wieck A D, Poggio M and Warburton R J 2013 *Nat. Phys.* **9** 570
[27] Crooker S A, Brandt J, Sandfort C, Greilich A, Yakovlev D R, Reuter D, Wieck A D and Bayer M 2010 *Phys. Rev. Lett.* **104** 036601
[28] Matthiesen C, Stanley M J, Hugues M, Clarke E and Atatüre M 2014 *Sci. Rep.* **4** 4911
[29] Lenhard A, Bock M, Becher C, Kucera S, Brito J, Eich P, Müller P and Eschner J 2015 *Phys. Rev.* A **92** 063827
[30] Trautmann N and Alber G 2016 *Phys. Rev.* A **93** 053807
[31] Yang S *et al* 2016 *Nat. Photon.* **10** 507
[32] Glaetzle A W, Hammerer K, Daley A J, Blatt R and Zoller P 2010 *Opt. Commun.* **283** 758
[33] Calajò G, Rizzuto L and Passante R 2017 *Phys. Rev.* A **96** 023802
[34] Budker D and Romalis M 2007 *Nat. Phys.* **3** 227

[35] Taylor J M, Cappellaro P, Childress L, Jiang L, Budker D, Hemmer P R, Yacoby A, Walsworth R and Lukin M D 2008 *Nat. Phys.* **4** 810
[36] Acosta V M, Bauch E, Jarmola A, Zipp L J, Ledbetter M P and Budker D 2010 *Appl. Phys. Lett.* **97** 174104
[37] Lee J-S, Rohrdanz M A and Khitrin A K 2008 *J. Phys. B: At. Mol. Opt. Phys.* **41** 045504
[38] Campos A G, Bondar D I, Cabrera R and Rabitz H A 2017 *Phys. Rev. Lett.* **118** 083201
[39] Fotso H F and Dobrovitski V V 2017 *Phys. Rev.* B **95** 214301
[40] Joas T, Waeber A M, Braunbeck G and Reinhard F 2017 *Nat. Commun.* **8** 964
[41] Uhrig G S 2007 *Phys. Rev. Lett.* **98** 100504
[42] Mollow B R 1969 *Phys. Rev.* **188** 1969
[43] Autler S H and Townes C H 1955 *Phys. Rev.* **100** 703
[44] Knight P L and Milonni P W 1980 *Phys. Rep.* **66** 21
[45] Cohen-Tannoudji C, Dupont-Roc J and Grynberg G 1992 *Atom-Photon Interactions, Basic Processes and Applications* (New York: Wiley)
[46] Jeener J and Henin F 1986 *Phys. Rev.* A **34** 4897 6
[47] Scully M O and Zubairy M S 1997 *Quantum Optics* (Cambridge: Cambridge University Press)
[48] Mollow B R 1972 *Phys. Rev.* A **3** 2217
[49] Mollow B R 1972 *Phys. Rev.* A **5** 1522
[50] Wu F Y, Ezekiel S, Ducloy M and Mollow B R 1977 *Phys. Rev. Lett.* **38** 1077
[51] Bloom S and Margenau H 1953 *Phys. Rev.* **90** 791